IDENTIFICATION OF GOLD MINERALIZATION ZONE USING MAGNETIC METHOD AND TIME DOMAIN INDUCED POLARIZATION METHOD ON CIPARAY BLOCK, CIBALIUNG, PANDEGLANG, BANTEN
(If exists, Title in Turkish) -MAKALE BAŞLIĞININ TÜRKÇESİ

Ribka Rebekka Marpaung[a][**], Alimuddin[a][*], Ordas Dewanto[a][***], Muhammad Arief Wicaksono[b][****], Andi Kurniawan[b][*****]

[a] Department of Geophysical Engineering, Faculty of Engineering, University of Lampung, Bandar Lampung, INDONESIA
[b] PT Aneka Tambang (Persero) Tbk, Jakarta, INDONESIA

ABSTRACT

Geologically, Indonesia is known to be rich in various types of minerals, one of which is gold. However, the content of mineral reserves is running low, while the demand for industry and investment interest on a local and global scale continue to increase, along with population growth and industrial development. Therefore, it is necessary to explore mineral resources using integrated geophysical methods supported by geological data to facilitate the identification of structures and alteration zones as controllers of gold mineralization zones, to meet the ever-increasing needs. So hopefully, research from this integrated method can be an option in the exploration of mineral resources, especially gold minerals. From the results of the integration between the magnetic response of the Magnetic method and the electrical response (resistivity and chargeability) of the Time Domain Induced Polarization method, the gold mineralization zone is at lane 1 and lane 2 in the direction of Southwest - Northeast Ciparay, lane 5, lane 6, lane 7, and lane 8 in the direction of Southwest Ciparay which is indicated by the value of high magnetic anomaly, high resistivity, and high chargeability, as well as the development of argillic alteration zones, namely illite and smectite.

ÖZ

Türkçe öz, Abstract ile birebir uyumlu olmalı ve 150 kelimeyi geçmemelidir.

Foreign authors may request help from our Editorial Board for the translation of Abstract and title of the paper into Turkish.

* Corresponding Author: alimuddin.geofisika@eng.unila.ac.id
** ribkarebekka22@gmail.com
*** ordas.dewanto@eng.unila.ac.id
**** wicaksonoarief123@gmail.com
***** andi.kurniawan@antam.com

INTRODUCTION

Indonesia is an area with three large tectonic plates, namely the Indo-Australian Plate, the Eurasian Plate, and the Pacific Plate. Indonesia is also part of the Ring of Fire lane, where it stretches between subduction and separation of the Pacific Plate with the Indo-Australian Plate, the Eurasian Plate, the North American Plate, and the Nazca Plate which crash with the South American Plate. This resulted in Indonesia having a complex tectonic order from the direction of the subduction zone, namely Fore Arc, Volcano Arc, and Back Arc. Where each of these regions has geological diversity and contains considerable potential natural resources of the mine. One of the mining resources, namely mineral resources.

The existence of mineral resources is affected by the process of magmatism, namely hydrothermal. The process of hydrothermal is closely related to the formation of sulfide ore mineralization. Hydrothermal mineralization formation system is a process of forming ore mineral deposits from the hot fluid (50°C - 500°C) laterally and vertically at various temperatures and pressures below the earth's surface. The effect of high temperature and pressure causes changes in the mineralogical composition of rocks which is a rock alteration process. The cause of the conversion of primary minerals into alteration minerals is because of the interaction between the hydrothermal fluid and the rocks through which it passes. One of the hydrothermal deposits, namely low sulfidation type epithermal deposits. Low sulfidation epithermal deposits are controlled by shifting structures and associate with rhyolitic volcanism.

Structural control is related to the formation of low sulfidation epithermal deposits, which are an important aspect in determining exploration using geophysical methods. The presence of low sulfide ore minerals in the mineralization zone becomes a parameter in determining the appropriate geophysical method. Sulfide ore minerals can be distinguished from magnetism and electricity resulting from induced polarization because metal minerals under normal conditions have a response of magnetism (susceptibility) and electricity (resistivity and chargeability) are high when compared to non-metallic minerals. So with physical parameters of the metal minerals, the magnetic method and the Time Domain Induced Polarization (TDIP) method can be used to find the delineation of the control structure and the mineralization zones of low sulfidation epithermal deposits.

The goals of this research are:
1. Identify the presence of structures based on 2D subsurface magnetic anomalies as a mineralization controller.
2. Identify structures and classify alteration zones based on 2D resistivity and chargeability as well as 3D resistivity and chargeability.
3. Identify mineralization zones based on the correlation between magnetic response and electrical response (resistivity and chargeability).

GEOLOGICAL SETTING

Java Island, a part of the eastern Sunda magmatic arc, is becoming an emerging part of the region for gold and copper endowment. A total of 15.4% of 1044 tons of Java gold endowment is originated from Low Sulfidation (LS) epithermal deposit type. The mineralization type that has given a significant credit to the gold endowment of Java is intriguing to be geologically evaluated (Carlile and Mitchell, 1994; Setijadji and Maryono, 2012; Prihatmoko and Idrus 2020)

This research area is in Java, which is located in the Southwest of Banten Province. This area has regional boundaries, namely:
- Northside is bordered by Tanjung Lesung and Citeureup
- Southside is bordered by the Indian Ocean
- Eastside is bordered by West Java Province
- Westside is bordered by Ujung Kulon National Park

The Cibaliung deposit is situated in the Miocene Honje Igneous Complex in the southwestern part of Java island approximately 70 km west of Bayah Dome (a gold district at western Java). The exploration work at the Cibaliung deposit have

delineated the extent of quartz veins approximately 1.4 km with an average width of about 10 m. Six meters width of the Cibaliung quartz vein outcrop was initially discovered at Cikoneng Creek. The metal resource has been reported amounting to 1.3 million tonnes at 10.42 g/t gold and 60.7 g/t silver at a 3 g/t Au cut-off (Carlile, et al., 2005; Prihatmoko and Idrus 2020). This equates to approximately 435,000 oz of gold and 2.54 million ounces of silver.

Regionally, the research area is composed of the Honje Formation located in the Southwest of Java Island. The Honje Formation is about 70 km to the west and separated from the Bayah Dome where the gold deposits of Mount Pongkor and Cikotok are located. The Honje Formation consists of basaltic and andesitic lava, volcanic breccias, agglomerates, lapilli tuffs, rhyolitic tuffs, and tuff breccias.

Basaltic lava is dark gray, sometimes porphyritic phenocrystalline plagioclase, very coarse in size. Andesitic lava is greenish-gray, porphyritic with a medium-sized plagioclase phenocryst, with a glass-bottom mass, interlocking between basalt lava, volcanic breccias or agglomerates. Volcanic breccias are dark gray, basalt fragmented with sandy tuff matrix, crust-sized fragments, angular responsibility. Aglomerates are dark gray to greenish, basalt and andesite fragments, porous-sized, rounded, angled. Breccias and glacial textured agglomerates. Lapilli tuffs are lytic containing andesite components, brownish-white, aligned bed structure, andesitic arrangement. Rhyolitic tuff is whitish gray, the structure of the bedding is parallel, fine-grained. Tuff breccias is greenish, tuff fragments with parallel layered structures, the size of the crust is angular.

The dip and strike of the northeast-southwest trending rocks with the dip towards the southeast. The Honje Formation is estimated to be of Middle Miocene age (Angeles, et al., 2002).
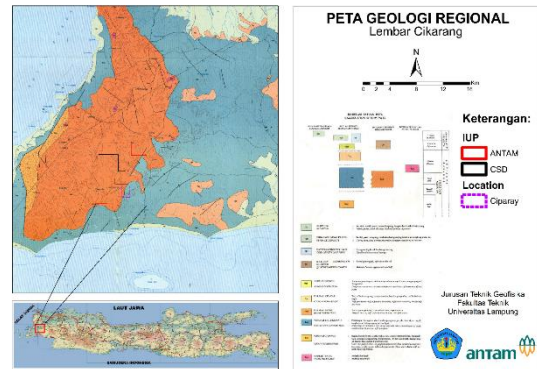
* Corresponding Author: alimuddin.geofisika@eng.unila.ac.id
** ribkarebekka22@gmail.com
*** ordas.dewanto@eng.unila.ac.id
**** wicaksonoarief123@gmail.com
***** andi.kurniawan@antam.com

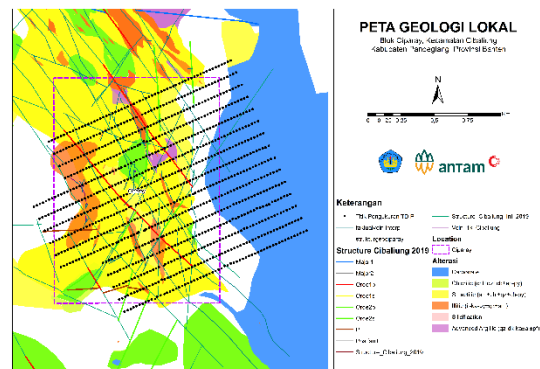**Photo 1.** Map of the Regional Geology of Cibaliung, Pandeglang, Banten

Photo 2. Local Geological Map of Ciparay Block

THEORY

Magnetic Method

The principle in investigation, magnetism is always considered that the magnetism of rocks that responds to magnetic measurements is only caused by the effect of magnetic induction. Thus, this magnetic nature is used as a basis in magnetic investigations. Whereas residual magnetism is generally neglected in magnetic investigations because besides the effect is very small, also to obtain the magnitude and direction of magnetism must be measured in a paleomagnetic laboratory using special tools. Changes that occur in the earth's magnetic field strength are very small and require a very long time to reach hundreds to thousands of years. Therefore, during a magnetic probe, the magnetic field strength is always considered constant. Assuming the strength of the earth's magnetic field (H) is constant, the magnitude of the earth's magnetic intensity (I) depends solely on variations

in the susceptibility of rock magnets that reflect the price of magnetic measurements. This principle is used as a basis in magnetic inquiry (Telford, et al., 1990).

Processing and Interpretation in Magnetic Data are as follows:

1. Diurnal Correctio

Diurnal correction is a deviation in the value of the earth's magnetic field due to differences in time and the effect of solar radiation in one day. The intended time must refer to or in accordance with the measurement time of the magnetic field data at each location point (measurement station) to be corrected. If the daily variation value is negative, then the daily correction is done by adding the daily variation value recorded at a certain time with the magnetic field data to be corrected. Otherwise, if the daily variation is positive, then the correction is done by subtracting the value of the daily variation recorded at a certain time of the magnetic field data to be corrected, can be written in the equation:

$$\Delta H = H_{total} \pm \Delta H_{harian}$$ .... (1)

2. IGRF Correction

The magnetic field measurement data is the contribution of three basic components, namely the Earth's main magnetic field, external magnetic field, and anomalous field. The value of the main magnetic field is none other than the IGRF value. If the value of the main magnetic field is removed by daily correction, the contribution of the main magnetic field is eliminated by the correction of IGRF. IGRF correction can be done by subtracting the IGRF value from the total magnetic field value that has been corrected daily at each measurement point at the appropriate geographical position. The correction equation (after diurnal correction) can be written as follows:

$$\Delta H = H_{total} \pm \Delta H_{harian} - H_0$$ .... (2)
Where: $H_0 = IGRF$

3. Reduction to The Pole

Reduction to the pole is the process of transforming anomalous magnetic fields from the measurement site into magnetic field anomalies north of the magnetic field. This needs to be done because there are a magnetic direction and variations in inclination and declination that cause the value of the magnetic anomaly to shift from the source of the anomaly, making it difficult to interpret the magnetic anomaly. The method of reduction to the Earth's magnetic pole can reduce one of the complicated stages of the interpretation process, where the magnetic field anomaly shows directly the object's position. The reduction transformation process to the poles is done by changing the direction of magnetization and the main field in the vertical direction, but it is still caused by the same source.

This reduction to the pole assumes that at all locations of data collection the value of the earth's magnetic field (especially Inclination and Declination) has a constant value and direction by making the inclination angle of the object 90° and the declination 0°. This assumption is accepted if the location has a relatively narrow area. But this cannot be accepted if the area of data collection is very wide because it involves varying latitude and longitude values, where the value of the earth's magnetic field changes gradually.

4. Analytic Signal

The analytic signal is a combination of derivative methods that can be expressed in the following equation:

$$|A(x,y)| = \sqrt{\left(\frac{\partial M}{\partial x}\right)^2 + \left(\frac{\partial M}{\partial y}\right)^2 + \left(\frac{\partial M}{\partial z}\right)^2}$$ .... (3)

The analytic signal can help interpret magnetic data because they can display maxima values right above the edge of the source body even when the direction of the body is not vertical. The analytic signal is completely independent of the direction of magnetization and the magnetic field of the earth, where all objects with the same geometry have the same analytic signal. Interpretation of signal maps and analytic images can provide an indication of the geometry of magnetic sources that is simple and easy to understand. This transformation is often useful at low magnetic latitudes due to problems inherent in RTP at low latitudes such as (Blakely, 1995).

The analytic signal can be useful to help the results of Reduction to The Pole which is not too good because the research location is in areas with low latitude. The analytic signal can show the dipole body on a magnetic anomaly becomes monopole.

5. First Horizontal Derivative

First horizontal derivative is used for the interpretation of magnetic data. This method is used to determine the subsurface structure of the study area. The horizontal derivative method is used to find the anomalous contrast boundaries of the data. The biggest advantage of the horizontal gradient method is that it is at least susceptible to noise in the data, requiring only the calculation of two first-order horizontal derivatives from the field and a horizontal gradient filter (Phillips and Hughes, 1998). Cordell and Grauch, 1985, state the amplitude of the horizontal gradient in the magnetic field are expressed by the equation:

$$HG(x, y) = \left[\left(\frac{\partial H}{\partial x}\right)^2 + \left(\frac{\partial H}{\partial y}\right)^2 \right]^{1/2} \quad .... (4)$$

where:
- $\frac{\partial H}{\partial x}$ dan $\frac{\partial H}{\partial y}$ is the horizontal derivative of the magnetic field in the x and y directions
- HG(x,y) is the horizontal derivative in the x and y directions

6. Second Vertical Derivative

Second Vertical Derivative is an interpretation technique that can help to highlight shallow sources. SVD can be used to describe the boundary of a body by interpreting the zero value as an outline of the body. The second vertical derivative of the magnetic field is the value of the change in the vertical direction in the form of the measure of potential field curvature, where a positive value indicates an increase in the vertical gradient and a negative value indicates a decrease in the vertical gradient of the potential field. For the calculation of the second derivative of magnetic anomalies used Laplace's mathematical equation which is stated as follows:

$$\nabla^2 \Delta T = 0 .... (5)$$

* Corresponding Author: alimuddin.geofisika@eng.unila.ac.id
** ribkarebekka22@gmail.com
*** ordas.dewanto@eng.unila.ac.id
**** wicaksonoarief123@gmail.com
***** andi.kurniawan@antam.com

$$\frac{\partial^2 \Delta T}{\partial x^2} + \frac{\partial^2 \Delta T}{\partial y^2} + \frac{\partial^2 \Delta T}{\partial z^2} = 0 .... (6)$$

So that the vertical derivative of both can be written as follows:

$$\frac{\partial^2 \Delta T}{\partial z^2} = -\left(\frac{\partial^2 \Delta T}{\partial x^2} + \frac{\partial^2 \Delta T}{\partial y^2} \right) .... (7)$$

For 1D (cross-section) data, the equation is as follows:

$$\frac{\partial^2 \Delta T}{\partial z^2} = -\frac{\partial^2 \Delta T}{\partial x^2} .... (8)$$

So from this equation, it is known that the value of the second vertical magnetic anomaly is equal to the negative value of the horizontal second derivative, where the minimum absolute value of the second derivative which is greater than the maximum absolute value will indicate the structure of the basin. While the maximum absolute value greater than the minimum absolute value of the second derivative will indicate the presence of intrusion structure. This can be seen in the following explanation:

1. For normal fault:
$$\left(\frac{\partial^2 \Delta T}{\partial z^2}\right)_{maks} > \left(\frac{\partial^2 \Delta T}{\partial z^2}\right)_{min} .... (9)$$

2. For reverse fault:
$$\left(\frac{\partial^2 \Delta T}{\partial z^2}\right)_{maks} < \left(\frac{\partial^2 \Delta T}{\partial z^2}\right)_{min} .... (10)$$

The magnetic method is used to determine variations in the magnetic field. Magnetic variation is caused by the inhomogeneous magnetic properties of the earth's crust, where rocks in the geothermal system generally have a lower magnetization than the surrounding rocks. This is due to the demagnetization process by the hydrothermal alteration process, in which the process converts existing minerals into paramagnetic or even diamagnetic minerals (Sumintadirejo, 2005; Indratmoko, et al., 2009).

Time Domain Induced Polarization Method
Induced Polarization Method is a method that can be used to investigate the structure of the earth's surface that contains mineral deposits. With the principle of flowing electric current into the earth then observing the potential difference that occurs after the electric current is stopped. When the

current is cut off, ideally the potential difference is immediately zero/lost, but in certain media will store electrical energy (as a capacitor) and will be released again. So, even though the current has been disconnected, but the voltage difference still exists will decay with time and gradually disappear. This effect is called the Induced Polarization Effect. Polarization can occur due to a medium containing metal minerals. The Induced Polarization method can identify disseminated minerals but it is difficult for massive minerals. This is because minerals that are dispersed are more easily polarized due to the current passing through them.

The principle of time domain is to measure differences in the response of rocks containing conductive minerals or not by looking at overvoltage (increase in potential difference) on rocks as a function of time due to the polarization effect. When the current is turned off, overvoltage delay per time is measured, so that the apparent chargeability (Ma) value will be obtained.
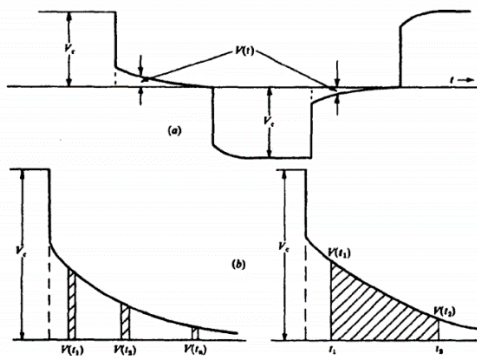

Photo 3. The concept of induced polarization measurement time area (Telford, et al., 1990)

Parameters calculated as a hint of polarization in the time domain are:
- The induced polarization effect is the simplest measurement, measuring the residual voltage at a certain time after the current is decided. The residual voltage at the time after the current is cut off in millivolts (mV), while normal voltage is in volts. The effect of the polarization induction effect is often expressed in millivolts/volts by comparison:

$$\text{IP Effect} = \frac{Vs}{Vp} \times 100 \dots\dots\dots\dots\dots\dots (11)$$

where:
Vs = secondary voltage, when (t) after the current is cut off
Vp = primary voltage

- Chargeability (M) is a measurement that is often used in the measurement of induced polarization with the time-domain method, chargeability (M) is obtained in units of milliseconds and expressed as:

$$M = \frac{1}{Vp} \int_{t1}^{t2} Vs(t) \, dt \dots\dots\dots\dots\dots (12)$$

Chargeability indicates how long the polarization effect will disappear shortly after the current has been turned off. So if the value of Ma is large, the time delay is long. And if the delay time is long, it can be assumed that conductive minerals are detected.

In theory, the results of Induced Polarization measurements in the time domain and frequency domain produce the same thing. Practically the conversion in the time domain to the frequency domain is quite difficult. The square wave used in the time domain contains all frequencies. In the book Telford, at al., 1990 was formulated:

$$M = \frac{FE}{(1+FE)} \dots\dots\dots\dots\dots\dots (13)$$

where FE<<1. MF parameters can also be used in the time domain, namely:

$$\text{Metal Factor (MF)} = \frac{1000M}{\rho} \dots\dots\dots (14)$$

where M is the value of chargeability (msec) and ρ is the resistivity value. Note that the time domain MF value is not always the same as the frequency domain MF value. The MF parameter is used to compensate for the Induced Polarization parameters against the price of the type prisoner.

Resistivity value is a value that shows the ability of a material to deliver electricity. Specific resistivity values can be described with rocks in

the following table:

Table 1. Rock Resistivity (Telford, et al., 1990)

Material	Resistivity (Ωm)
Air	~
Pyrite	0.01 – 100
Quartz	$500 – 8 \times 10^5$
Calcite	$1 \times 10^{12} – 1 \times 10^{13}$
Rock Salt	$30 – 1 \times 10^{13}$
Granite	$200 – 1 \times 10^5$
Andesite	$1.7 \times 10^2 – 4.5 \times 10^4$
Basalt	$10 – 1.3 \times 10^7$
Limestone	$500 – 1 \times 10^4$
Sandstone	200 – 8000
Rock Flakes	20 – 2000
Sand	1 – 1000
Clay	1 – 100
Groundwater	0.5 – 300
Sea Water	0.2
Magnetite	0.01 – 1000
Dry Gravel	600 – 1000
Aluvium	10 – 800
Gravel	100 – 600

Whereas the chargeability data is a decrease in potential difference when the current is turned off (t0) until the current returns to 0 (t1) and is used to determine the mineral content of the rock. Where the value of chargeability depends on the spread or diffusion of ions into metal minerals and the movement of ions in the pore-filling electrolyte. So that the higher chargeability value is, the greater the potential of the area is sulfide minerals. The following table shows the variation of rock chargeability values.

Table 2. Mineral Chargeability (Telford, et al., 1990)

Mineral	Chargeability (ms)
Pyrite	13.4
Chalcocite	13.2
Copper	12.3
Graphite	11.2
Chalcopyrite	9.4
Bornite	6.3
Galena	3.7
Magnetite	2.2
Malachite	0.2
Hematite	0.0

* Corresponding Author: alimuddin.geofisika@eng.unila.ac.id
** ribkarebekka22@gmail.com
*** ordas.dewanto@eng.unila.ac.id
**** wicaksonoarief123@gmail.com
***** andi.kurniawan@antam.com

Hydrothermal is a residual fluid of magma that is "aqueous" as a result of magma differentiation. This hydrothermal is rich with relatively light metals, and is the largest source (90%) of the process of deposition. Based on the method of sediment formation, there are two types of hydrothermal deposits, namely:

1. Cavity filling, filling holes (openings) that are already in the rock.
2. Metasomatism, replacing the elements that already exist in rocks with new elements from a hydrothermal fluid.

The hydrothermal system is defined as circulating hot fluid (50°C - 500°C), laterally and vertically at varying temperatures and pressures the subsurface. This system contains two main components, namely heat source, and fluid phase. Circulation of hydrothermal fluid causes mineral deposits in wall rocks to become unstable and tends to adjust the new equilibrium by forming mineral assemblies following new conditions, known as hydrothermal alterations. Hydrothermal mineral deposits can be formed due to the circulation of hydrothermal fluids that leach, transport, and precipitate new minerals in response to physical and chemical changes (Pirajno, 1992; Sutarto, 2004).

Hydrothermal fluid in geothermal systems causes massive changes in the chemical and physical properties of subsurface rocks, including the magnetic properties of rocks. The susceptibility value becomes lower at higher temperatures so that the magnetization given by the material response becomes lower. Magnetization in these rocks has decreased due to heating activity by geothermal sources (Chen, et al., 2013).

The hydrothermal fluid is formed in the final phase of the magma freezing cycle. The interaction between the hydrothermal and the rocks that are passed through will cause the alteration of the side rock constituent minerals and form alteration minerals. The hydrothermal fluid will be deposited somewhere forming mineralization (Bateman, 1981).

The dominant factors that effect mineral deposition in the hydrothermal system consist of four types (Barnes, 1979; Guilbert and Park, 1986), namely:

1. Changes in temperature
2. Changes in pressure
3. Chemical reactions between hydrothermal fluid and rocks being passed through
4. Mixing between two different fluid.

Fluid temperature and pH are the most important factors affecting the hydrothermal system mineralogy. The pressure is directly related to temperature, and elemental concentration is expressed in the pH of mineralized rocks (Corbett and Leach, 1997).
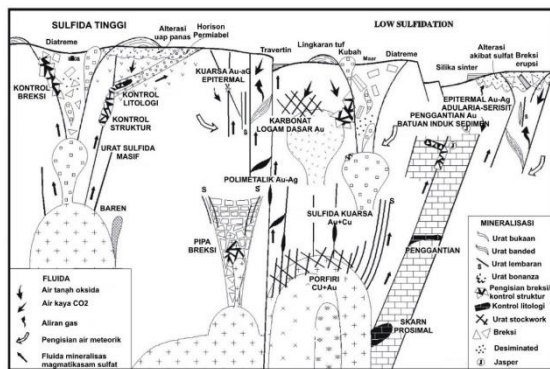

Photo 4. Gold-silver mineralization model of the Pacific Rim (Corbett, 2002)

Hydrothermal Mineralization

Mineralization is a process of deposition of ore minerals (metal) from the media that carries it due to changes in the surrounding chemical and physical environment.

Mineralization formation systems in the Pacific circle generally consist of porphyry, mesothermal to epithermal type deposits (Corbett and Leach, 1997).

Porphyry and epithermal ore deposits of high-, intermediate and low sulfidation styles (HS, IS and LS, respectively) are related to the generation of hydrous calc-alkaline and alkaline magmas in both subduction and post subduction settings (Seedorff, et al., 2005; Sillitoe, 2010; Richards, 2009, 2011; Kouzmanov and Pokrovski, 2012; Voudouris, P, et al., 2019).

Porphyry types are formed at depths greater than 1 km and source rocks are intrusive rocks. Sillitoe, 1993; Corbett and Leach, 1997, suggested that porphyry deposits have a diameter of 1 to >2 km and are cylindrical.

The mesothermal type is formed at medium temperature and pressure and has a temperature of >300ºC (Lindgren, 1922; Corbett and Leach, 1997). The sulfide content of the ore consists of chalcopyrite, sphalerite, galena, tetrahedrite, bornite, and calcocytes. The accompanying minerals consist of quartz, carbonate (calcite, siderite, rococrocite), and pyrite. Alteration minerals consist of sericite, quartz, calcite, dolomite, pyrite, orthoclasts, and clays.

Epithermal types are formed in shallow environments with temperatures <300ºC, and hydrothermal fluids are interpreted as sourced from meteoric fluids. This type of deposition is a continuation of the porphyry type hydrothermal system and is formed in the inner magmatic arc in calc-alkaline volcanic environments or sedimentary bedrock (Heyba et al., 1985; Corbett and Leach, 1997). These systems generally have variations in low sulfide and high sulfide deposits (**Photo 5**). Ore minerals consist of thymonidsulfate, arsenic sulfate, gold and silver, stibnite, argentite, cinnabar, electrum, pure gold, pure silver, selenide, and contain little galena, sphalerite, and galena. The accompanying minerals consist of quartz, amethyst, adularia, calcite, rheocrocite, barite, fluorite, and hematite. Alteration minerals consist of chlorite, sericite, alunite, zeolite, adularia, silica, pyrite, and calcite.
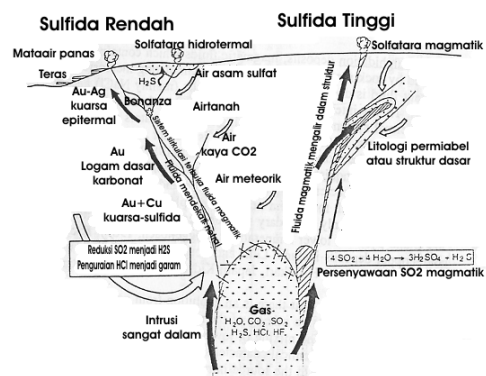

Photo 5. High and low sulfide fluid models (Corbett dan Leach, 1997)

Hydrothermal alteration

Alteration is a change in the composition of rock mineralogy (in a solid-state) due to the effect of high temperature and pressure and not in isochemical conditions producing clay minerals, quartz, oxide or metal sulfides. An alteration process is a secondary event, in contrast to the metamorphism which is a primary event. Alteration occurs in the intrusion of igneous rocks that experience heating and in certain structures that allow the entry of meteoric water to be able to change the mineralogical composition of rocks. Hydrothermal alteration is a very complex process that involves changes in mineralogy, chemistry, and texture caused by the interaction of hot fluids with the rocks in its path, under conditions of physio-chemical evolution. An alteration process is a form of metasomatism, namely the exchange of chemical components between liquids and wall rocks (Pirajno, 1992).

Interaction between hydrothermal fluid with the rocks that pass through it (wall rocks), will cause the conversion of primary minerals into alteration minerals, as well as the fluid itself (Pirajno, 1992; Sutarto, 2004).

The hydrothermal alteration will depend on:
1. The character of wall rock.
2. The character of fluid (eH, pH).
3. Pressure and temperature conditions at the time of the reaction (Guilbert and Park, 1986; Sutarto, 2004).
4. Concentration.
5. Duration of hydrothermal activity (Browne, 1991; Sutarto, 2004).

Although the factors above are interrelated, temperature and fluid chemistry are probably the most influential factors in the hydrothermal alteration process (Corbett and Leach, 1997; Sutarto, 2004). Henley and Ellis, 1983; Sutarto, 2004, believed that hydrothermal alteration in the epithermal system does not depend much on the composition of rock walls, but is more controlled by rock graduation, temperature, and fluid composition. Wall rock/country rock is the rock around the intrusion that surrounds the veins, generally undergoing hydrothermal alteration.

* Corresponding Author: alimuddin.geofisika@eng.unila.ac.id
** ribkarebekka22@gmail.com
*** ordas.dewanto@eng.unila.ac.id
**** wicaksonoarief123@gmail.com
***** andi.kurniawan@antam.com

The degree and duration of the alteration process will cause differences in alteration intensity and degree of alteration (related to the stability of formation). The stability of primary minerals undergoing alteration often forms a style of alteration in rocks (Pirajno, 1992; Sutarto, 2004). At a certain equilibrium, the hydrothermal process will produce certain mineral assemblages known as assemblage minerals (Guilbert and Park, 1986, in Sutarto, 2004). Each mineral set will reflect the type of alteration. A mineral with certain minerals is often found together (mineral associations), although they have different levels of formation stability, for example, chlorite is often associated with pyroxene or biotite. Areas showing the spread of similarities in the present mineral set can be united as one alteration zone. The host rock is a rock containing ore deposits or a rock that can be passed through a fluid, where an ore deposit is formed. Intrusion and wall rock can act as the host rock.

Photo 6. Relationship of alteration with mineralization in epithermal deposit types (Guilbert and Park, 1986).

Hydrothermal alteration is a process of mineral change due to several factors including temperature, fluid chemical composition, concentration/sensitivity, the composition of the host rock, duration of activity/degree of equilibrium, and permeability of the alteration zone (Corbett and Leach, 1997).

There are several types of alteration zones that describe the presence of a certain set of minerals in a rock that is seen based on the same equilibrium conditions and the following pH degrees.

Table 3. Alteration types are based on mineral assemblages (Guilbert, et al., 1986)

Tipe	Mineral Kunci	Mineral Asesoris	Keterangan
Propylitic	Chlorite, Epidote, Carbonate	Albit, Quartz, Calcite, Pyrite, Clay/illite, Iron Oxide	Temperature 200º-300ºC, salinity varies, pH approaches neutral, area with low permeability
Argilic	Smectite, Monmorillonite, Illite-smectite, Kaolinite	Pyrite, Clorite, Calcite, Quartz	Temperature 100º-300ºC, low salinity, acidic-neutral pH
Advanced Argillic (*low temperature*)	Kaolinite, Alunite	Chalcedon, Cristobalite, Quartz, Pyrite	Temperature 180ºC, acidic pH
Advanced Argillic (*high temperature*)	Pirofilite, Diaspor, Andalusite	Quartz, Tourmaline, Enargit, Luzonite	Temperature 250º-350ºC
Potassic	Adularia, Biotite, Quartz	Chlorite, Epidot, Pyrite, Illite-sericite	Temperature > 300ºC, high salinity, close to intrusive rocks
Pyilic	Quartz, Sericite, Pyrite	Anhydrite, Pyrite, Calsite, Rutile	Temperature 230º-400ºC, salinity varies, acidic-neutral pH, permeable zone at the vein

METHODS

1. Magnetic Data Collection

Magnetic data is measurement data that contains magnetic intensity values, point coordinates, and point measurements. In this study, data collection was carried out on 15 measurement trajectories with 4460 measured data, and later corrections were made to determine the rock's susceptibility response so that structure identification could be carried out as a controller for alteration zones and mineralization zones.

2. Time Domain Induced Polarization (TDIP)

Data collection Time Domain Induced Polarization (TDIP) data is measurement data that contains datum points, offset values, apparent resistivity values, and apparent chargeability values. In this study, data collection was carried out on 15 measurement trajectories with 493 measured data which will later be made from these data corrections to determine the electrical response (actual resistivity and actual chargeability) of rocks so that identification of structures, alteration zones, and mineralization zones.

3. Structure Identification

Data that has been collected is processed by the analytic signal magnetic method and sees the resistivity value of the TDIP method which is between high and low contrast to determine the direction of the structure and the presence of structures on Ciparay block, Cibaliung, Pandeglang, Banten. At this stage will also find that the rocks are strongly altered and unaltered from the value of the magnetic response (susceptibility) and the resistivity value which is correlated with the value of the chargeability.

4. Identification of Alteration Types

After knowing the direction of the structure and its existence, it is continued by identifying the types of alterations found in the study area by looking at the electrical values that are correlated with each other in the study area to be integrated with the data reduction to the poles of the magnetic method which has a low response value (susceptibility). At this stage also carried out modeling of each type of alteration that was identified based on the magnetic value and the electrical value of rocks contained on Ciparay block, Cibaliung, Pandeglang, Banten.

5. Identification of Mineralized Zones

After knowing the structure and type of alteration contained in the study area, then proceed to identify the mineralization zone by looking at the correlation of the actual resistivity value and the actual chargeability value that is right in the structure as a controller of the mineralization zone and alteration zone. At this stage, a mineralization zone modeled for veinlets identified was identified based on magnetic values, electrical values, and structural controls found on Ciparay block, Cibaliung, Pandeglang, Banten.

DISCUSSION

Structure Analysis Using Magnetic Data

Measurement data contains magnetic intensity values, point coordinates, and measurement points that have been done diurnal correction, then IGRF correction to eliminate the effect of the earth's main magnetic field, so that the value obtained is only the local anomalous magnetic field value. The IGRF value used was 44723.1 nT. IGRF correction is done by subtracting the value of the diurnal corrected magnetic field with the reference value of the earth's main magnetic field as shown in **Photo 7**.

After IGRF correction, the next processing process is the process of making magnetic anomaly contour maps starting from the data gridding stage using the minimum curvature gridding method in Oasis Montaj Software 8.4.4. The data that has been carried out by the gridding process produces a total magnetic anomaly contour map.

The contours of the magnetic anomaly intensity in **Photo 8.** show the distribution of anomaly intensity values that vary from high values (pink) to low values (blue). This variation of magnetic anomaly value has a maximum intensity value of magnetic anomaly, which is 78.3 nT and a minimum intensity value of magnetic anomaly, which is -202.4 nT. The contours of the intensity of the magnetic anomaly are transformed to the poles (RTP) to position the magnetic anomaly in

the right direction below the surface to be vertical, with correction inclination angles of -29.26083333°, declination angles of 0.5175°, and amplitude correction values of -60.73916667°.

The contours of the intensity of the magnetic anomaly after the Reduce to Magnetic Pole process in **Photo 9.** show a lateral strengthening of the anomalous intensity. The contours of the magnetic anomaly intensity before the RTP showed high-intensity values scattered with intensity values ranging from -34.8 nT to 78.3 nT. The low-intensity distribution is also spread with intensity values ranging from -114.7 nT to -202.4 nT. On the RTP contour, the value of the high magnetic intensity distribution is concentrated in the northwest with values ranging from -26.0 nT to 91.2 nT. The distribution of low magnetic intensity values is also centered on the Southeast, with values ranging from -124.6 nT to -232.4 nT.

After the RTP is done, the next process is to filter Analytic Signal, First Horizontal Derivative, and Second Vertical Derivative. Analytic Signal is useful to help the results of Reduce to Magnetic Pole which is not too good because the research location is in areas with low latitude. Analytic Signal can show that a body dipole in a magnetic anomaly becomes a monopoly. First Horizontal Derivative is useful for finding the anomalous contrast boundaries of the data. Second Vertical Derivative is used to describe the boundary of a body by interpreting the zero value as an outline of the body. Contour maps of Analytic Signal, First Horizontal Derivative, and Second Vertical Derivative can be seen in **Photo 10, Photo 11, and Photo 12**.

Analytic Signal will eliminate the negative effects of previous processing, so the value obtained is always positive. As shown in **Photo 10.** High amplitude values have values ranging from 2.3 to 6.9 and low amplitude values have values ranging from 0.2 to 0.1.

Just like Analytic Signal, First Horizontal Derivative will eliminate the negative effects of previous processing, so the value obtained is always positive. As shown in **Photo 11.** High

* Corresponding Author: alimuddin.geofisika@eng.unila.ac.id
** ribkarebekka22@gmail.com
*** ordas.dewanto@eng.unila.ac.id
**** wicaksonoarief123@gmail.com
***** andi.kurniawan@antam.com

amplitude values have values ranging from 1.4 to 4.1 and low amplitude values have values ranging from 0.1 to 0.

Second Vertical Derivative of the magnetic field is the value of the gradient changes in the vertical direction in the form of measurement of the curvature of the potential field, where a positive value indicates an increase in the vertical gradient and a negative value indicates a decrease in the vertical gradient of the potential field. As shown in **Photo 12.** High amplitude values have values ranging from 0 to 0.2 and low amplitude values have values ranging from -0.0 to -0.2.

Furthermore, from the Analytic Signal, First Horizontal Derivative, and Second Vertical Derivative processes, identification of the structure is done by doing the slicing process 15 times as shown in **Photo 13**, where slicing is done to determine the amplitude value formed by the magnetic source. The maximum value in Analytic Signal and First Horizontal Derivative is indicated as the location of the structure's existence, while the zero value in the Second Vertical Derivative is to determine the existence and type of structure.

The process of slicing on the contours of Analytic Signal, First Horizontal Derivative, and Second Vertical Derivative as shown in **Photo 13.** is done at the same point to get a correlated result between Analytic Signal, First Horizontal Derivative, and Second Vertical Derivative.

From the sliced results of **Photo 13.** correlated, points were obtained for the structure as seen in **Photo 14.** making it easier to interpret the delineation of the structure in the study area.

From the structural points obtained through the slicing process, it will be easy to determine the structural delineation in the study area as shown in **Photo 15.** where the structure in the study area is predominantly directed to the Northwest - Southeast.

After knowing the existence of the structure in the study area, then further determine the type of structure using the Second Vertical Derivative

filter by looking at the maximum value and minimum value between zero values as the body structure as **Photo 16.** and **Photo 17.**

Based on **Photo 16.** it can be seen that the first structure has a maximum absolute value (0.048056287) which is smaller than the absolute minimum value (0.054034605) so that the structure is a reverse fault. Furthermore, the second structure has a maximum absolute value (0.014236274) which is smaller than the minimum absolute value (0.055755668), so that the structure is a reverse fault. The third structure has a maximum absolute value (0.01350637) which is greater than the minimum absolute value (0.006733634), so the structure is a normal fault. Furthermore, the fourth structure has a maximum absolute value (0.030540707) which is smaller than the minimum absolute value (0.067275647), so that the structure is a reverse fault. The fifth structure has a maximum absolute value (0.034507698) that is greater than the minimum absolute value (0.012699521), so the structure is a normal fault. Furthermore, the sixth structure has a maximum absolute value (0.026038746) which is smaller than the minimum absolute value (0.052463059), so that the structure is a reverse fault. The seventh structure has a maximum absolute value (0.0870668) which is greater than the minimum absolute value (0.072505264), so the structure is a normal fault. Furthermore, the eighth structure has a maximum absolute value (0.025313073) which is greater than the minimum absolute value (0.00157066), so the structure is a normal fault. The ninth structure has a maximum absolute value (0.025313073) which is smaller than the minimum absolute value (0.026152314), so the structure is a reverse fault. And for the last structure has a maximum absolute value (0.007242576) which is smaller than the minimum absolute value (0.010687919), so the structure is a reverse fault.

Based on **Photo 17.** it can be seen that the first structure has a maximum absolute value (0.101143396) which is smaller than the minimum absolute value (0.14792824) so that the structure is a reverse fault. Furthermore, the second structure has a maximum absolute value

(0.02586103) which is smaller than the minimum absolute value (0.048406591), so that the structure is a reverse fault. The third structure has a maximum absolute value (0.117623362) which is greater than the minimum absolute value (0.011739004), so the structure is a normal fault. Furthermore, the fourth structure has a maximum absolute value (0.417429353) which is greater than the absolute value (0.024773149), so the structure is a normal fault. The fifth structure has a maximum absolute value (0.087389474) which is smaller than the minimum absolute value (0.119943128), so the structure is a reverse fault. Furthermore, the sixth structure has a maximum absolute value (0.012758353) which is smaller than the minimum absolute value (0.048936642), so that the structure is a reverse fault. The seventh structure has a maximum absolute value (0.022931702) which is greater than the minimum absolute value (0.017841154), so the structure is a normal fault. And for the last structure has a maximum absolute value (0.03721463) which is greater than the minimum absolute value (0.002221002), so the structure is a normal fault.

Analysis of Structure and Alteration Zones Using Time Domain Induced Polarization Data
The data from Time Domain Induced Polarization measurement results are in the form of apparent resistivity and apparent chargeability. The data must be processed to obtain the true resistivity and true chargeability values. Data processing is performed using RES2DINV by doing Exterminate Bad Datum Points, which is removing bad datum points because the datum points have incorrect resistivity values. This could be due to electrode misalignment, poor contact of electrodes due to dry soil, or short circuit via cables due to very wet soil conditions. These datum points usually have apparent resistivity that is too large or too small compared to neighboring data.

Before carrying out the inversion process, the initial settings must be determined for the damping factor and other variables, so that the best results will be obtained by modifying the parameters that control the inversion process. The author sets the Damping Factors that are useful for setting the initial value of the damping factor. If the data has a lot of noise, you can use a relatively large damping factor (for example 0.3). If the data has little noise, then use a relatively small initial damping factor (for example 0.1). The inversion process will reduce the damping factor for the next iteration.

Next, the inversion process is carried out using Robust inversion. Robust inversion shows very well the result of boundary resolution between layers that are not affected by the type of configuration used when retrieving data. Thus, Robust inversion can provide optimal results for subsurface geology consisting of a homogeneous material with sharp boundaries between materials.

After completing the inversion process, the inversion results are obtained in the form of true resistivity and true chargeability values. Resistivity value is a value that shows the ability of a rock to conduct electricity. While the value of chargeability depends on the spread or diffusion of ions into metal minerals and the movement of ions in the pore-filling electrolyte. Thus, if the chargeability value is higher, the greater the potential of the area to have sulfide minerals. The variation of resistivity values obtained in the study area, namely from the value 0 - 1433.2 ohm.m and the variation of the value of the chargeability obtained in the study area, the value 0 - 810 msec, as shown in **Photo 18.** and **Photo 19**.

Based on 2D resistivity inversion results such as **Photo 18**, shows the contrast between the high and low resistivity values that continue from the first path to the last path, also shows the emergence of high resistivity values when on the surface and disappears at a certain depth, then reappears at deeper depths, where it shows the existence of a continuous structure in the study area. The presence of sulfide minerals in the study area can be identified through the presence of structures that act as hydrothermal fluid paths (heat sources).

And also based on the results of 2D inversion of resistivity and chargeability in correlation (**Photo 18.** and **Photo 19.**) can classify rocks and

* Corresponding Author: alimuddin.geofisika@eng.unila.ac.id
** ribkarebekka22@gmail.com
*** ordas.dewanto@eng.unila.ac.id
**** wicaksonoarief123@gmail.com
***** andi.kurniawan@antam.com

alterations found in the study area, as in **Table 7.** and **Table 8**.

Table 4. Classification of Resistivity and Chargeability Values

Scale	Resistivity (ohm.m)	Chargeability (msec)
Low	<14	<10
Medium	14 - 24	10 – 50.005
High	>24	>50.005

Table 5. Reference Interpretation Based on The Value of Resistivity and Chargeability

Interpretation	Resistivity	Chargeability
Argillic Alteration Zone	Low	Medium – High
Propylytic Alteration Zone	Medium – High	Medium – High
Gold Mineralization Zone	Medium – High	Medium – High
Intrusion Rocks	High	Low – Medium
Clay, Sandstone	Low	Low
Tuff	Medium – High	Medium – High

Based on **Table 4.** and **Table 5.** it can be described that the relatively low resistivity value (<14 ohm.m) and medium to high chargeability values (>10 msec) are indicated as strong alteration zones, namely argillic alteration zones with mineral sulfide content. When classified more specifically based on the geology of the study area, the alteration of the argillic zone can be divided into two, namely the smectite alteration and the illite alteration. Illite is a typical low temperature alteration mineral. Illite can be used to study the state of a hydrothermal deposit formation environment and as an indicator of the fluid properties, water/rock ratios, and mineral alterations (Pollastro, 1993; Velde, 1992; Guo, N., et al., 2019). Relatively high resistivity values (>24 ohm.m) and relatively low to medium chargeability values (<50.005 msec) indicate intrusion rocks. Relatively low resistivity (<14 ohm.m) and relatively low chargeability (<10 msec) indicate that there is clay in the area. Resistivity values that are relatively medium to high (>14 ohm.m) and relatively medium to high chargeability values (>10 msec) indicate that there are tuffs in the area.

Resistivity values that are also relatively medium to high (>14 ohm.m) and chargeability values that are also relatively medium to high (>10 msec) indicate that in that area is a propylitic alteration zone.

After completing the 2D resistivity and chargeability inversion, then modeling the 3D resistivity and chargeability of the 2D resistivity and chargeability inversion results using the Oasis Montaj Software 8.4.4. as seen in **Photo 20.** and **Photo 21**.

Based on **Photo 20.** and **Photo 21.** can be seen in more detail and specific continuity of the existing structure in the study area and also the alteration zone that exists by correlating the value of resistivity and chargeability.

Correlation Between Geological Data, Magnetic Data and Time Domain Induced Polarization Data in Determining the Gold Mineralization Zone

The results obtained from magnetic data and Time Domain Induced Polarization data supported by geological data show linkage to the interpretation of structures and alteration zones as controllers of mineralization zones. It is known that low magnetic anomaly values correlate with strongly altered environments. This happens because of the heat from the hydrothermal solution and the pH of the solution. This is justified by the Time Domain Induced Polarization data which has relatively low resistivity values (<14 ohm.m) which shows the presence of sulfide minerals.

When the resistivity value shows high values (>24 ohm.m) is an intrusive body response in the form of igneous rock which is very compact, then the ability to conduct electricity is low, which means it has relatively low chargeability values (<10 msec). Relatively high chargeability values (>50,005 msec) indicates the presence of sulfide minerals associated with gold.

The results of magnetic interpretation using analytic signals, first horizontal derivatives, and second vertical derivatives indicate a continuous structure in the research area. This is justified by

Time Domain Induced Polarization data when the correlation of the two data is performed.

Correlation between magnetic response and electrical response (resistivity and chargeability), the gold mineralization zone is in 1st lane and 2nd lane between a distance of 600 m to 800 m measurement in the Southwest - Northeast direction and also in 5th lane and 6th lane in between a distance of 0 m to 200 m measurement in the Southwest direction, 7th lane is on the measurement pole 0 m, and 8th lane between a distance of -200 m to 0 m measurement in the Southwest direction indicated by the value of high magnetic anomaly, high resistivity, and high chargeability, and the development of argillic alteration zones, namely illite, and smectite.

The first lane is based on the correlation between magnetic data using analytic signal filters, first horizontal derivatives, and second vertical derivatives and Time Domain Induced Polarization data with resistivity and chargeability parameters supported by geological data, the existence of structures that are represented by pull the dotted line as shown in **Photo 22.** And also based on **Photo 22.** can be classified alteration zones that develop on this lane. As seen in **Photo 22.** when relatively low resistivity values (<14 ohm.m) and medium to high chargeability values (>10 msec) indicated as a strong alteration zone indicate an argillic alteration zone. If classified more specifically based on the geology of the study area, the alteration of the argillic zone can be divided into two, namely the illite alteration and the smectite alteration. Relatively high resistivity values (>24 ohm.m) and relatively low to medium chargeability values (<50,005 msec) indicate intrusion rocks. Resistivity values that are relatively medium to high (>14 ohms.m) and relatively medium to high chargeability values (>10 msec) indicate that there are tuffs in the area.

The first lane has a mineral zone between the 700m - 725m measurement benchmarks, due to a continuous structure based on the correlation between the filter analytic signal, first horizontal derivative, and second vertical derivative and relatively medium to high resistivity values (>14 ohm.m) and relatively medium to high chargeability values (>10 msec) which indicates that there is a mineral zone on this lane.

The second lane is based on the correlation between magnetic data using analytic signal filters, first horizontal derivatives, and second vertical derivatives and Time Domain Induced Polarization data with resistivity and chargeability parameters supported by geological data, the existence of structures that are represented by pull the dotted line as shown in **Photo 23.** And also based on **Photo 23.** can be classified alteration zones that develop on this lane. As seen in **Photo 23.** when relatively low resistivity values (<14 ohm.m) and medium to high chargeability values (>10 msec) indicated as a strong alteration zone indicate an argillic alteration zone. If classified more specifically based on the geology of the study area, the alteration of the argillic zone can be divided into two, namely the illite alteration and the smectite alteration. Relatively high resistivity values (>24 ohm.m) and relatively low to medium chargeability values (<50,005 msec) indicate intrusion rocks. Resistivity values that are relatively medium to high (>14 ohms.m) and relatively medium to high chargeability values (>10 msec) indicate that there are tuffs in the area. Relatively low resistivity (<14 ohm.m) and relatively low chargeability (<10 msec) indicate that there is clay in the area.

The second lane has a mineral zone between the 650m - 700m measurement benchmarks, due to a continuous structure based on the correlation between the filter analytic signal, first horizontal derivative, and second vertical derivative and relatively medium to high resistivity values (>14 ohm.m) and relatively medium to high chargeability values (>35,005 msec) which indicates that there is a mineral zone on this lane.

The fifth lane is based on the correlation between magnetic data using analytic signal filters, first horizontal derivatives, and second vertical derivatives and Time Domain Induced Polarization data with resistivity and chargeability parameters supported by geological data, the existence of structures that are represented by

* Corresponding Author: alimuddin.geofisika@eng.unila.ac.id
** ribkarebekka22@gmail.com
*** ordas.dewanto@eng.unila.ac.id
**** wicaksonoarief123@gmail.com
***** andi.kurniawan@antam.com

pull the dotted line as shown in **Photo 24.** And also based on **Photo 24.** can be classified alteration zones that develop on this lane. As seen in **Photo 24.** when relatively low resistivity values (<14 ohm.m) and medium to high chargeability values (>10 msec) indicated as a strong alteration zone indicate an argillic alteration zone. If classified more specifically based on the geology of the research area, the alteration of the argillic zone can be divided into two, namely the illite alteration and the smectite alteration. Relatively medium to high resistivity (>14 ohm.m) and relatively medium to high chargeability values (>10 msec) indicate propylitic alteration. Relatively high resistivity values (>24 ohm.m) and relatively low to moderate chargeability values (<50,005 msec) indicate intrusion rocks.

The fifth lane has a mineral zone between the 100m - 125m measurement benchmarks, due to a continuous structure based on the correlation between the filter analytic signal, first horizontal derivative, and second vertical derivative and relatively medium to high resistivity values (>14 ohm.m) and relatively medium to high chargeability values (>15 msec) which indicates that there is a mineral zone on this lane.

The sixth lane is based on the correlation between magnetic data using analytic signal filters, first horizontal derivatives, and second vertical derivatives and Time Domain Induced Polarization data with resistivity and chargeability parameters supported by geological data, the existence of structures that are represented by pull the dotted line as shown in **Photo 25.** And also based on **Photo 25.** can be classified alteration zones that develop on this lane. As seen in **Photo 25.** when relatively low resistivity values (<14 ohm.m) and medium to high chargeability values (>10 msec) indicated as a strong alteration zone indicate an argillic alteration zone. If classified more specifically based on the geology of the research area, the alteration of the argillic zone can be divided into two, namely the illite alteration and the smectite alteration. Relatively medium to high resistivity (>14 ohm.m) and relatively medium to high chargeability values (>10 msec) indicate propylitic alteration.

Relatively high resistivity values (>24 ohm.m) and relatively low to medium chargeability values (<50,005 msec) indicate intrusion rocks. Relatively low resistivity (<14 ohm.m) and relatively low chargeability (<10 msec) indicate that there is clay in the area.

The sixth lane has a mineral zone between the 25m - 200m measurement benchmarks, due to a continuous structure based on the correlation between the filter analytic signal, first horizontal derivative, and second vertical derivative and relatively medium to high resistivity values (>14 ohm.m) and relatively medium to high chargeability values (>15 msec) which indicates that there is a mineral zone on this lane.

The seventh lane is based on the correlation between magnetic data using analytic signal filters, first horizontal derivatives, and second vertical derivatives and Time Domain Induced Polarization data with resistivity and chargeability parameters supported by geological data, the existence of structures that are represented by pull the dotted line as shown in **Photo 26.** And also based on **Photo 26.** can be classified alteration zones that develop on this lane. As seen in **Photo 26.** when relatively low resistivity values (<14 ohm.m) and medium to high chargeability values (>10 msec) indicated as a strong alteration zone indicate an argillic alteration zone. When classified more specifically based on the geology of the study area, the alteration of the argillic zone can be divided into two, namely the smectite alteration and the illite alteration. Relatively high resistivity values (>24 ohm.m) and relatively low to moderate chargeability values (<50,005 msec) indicate intrusion rocks. Relatively low resistivity (<14 ohm.m) and relatively low chargeability (<10 msec) indicate that there is clay in the area.

The seventh lane has a mineral zone between the 0m - 25m measurement benchmarks, due to the continuous structure based on the correlation between the filter analytic signal, first horizontal derivative, and second vertical derivative as well as relatively medium to high resistivity values (>14 ohm.m) and relatively medium to high

chargeability values (>10 msec) which indicates that there is a mineral zone on this lane.

The eighth lane is based on the correlation between magnetic data using analytic signal filters, first horizontal derivatives, and second vertical derivatives and Time Domain Induced Polarization data with resistivity and chargeability parameters supported by geological data, the existence of structures that are represented by pull the dotted line as shown in **Photo 27.** And also based on **Photo 27.** can be classified alteration zones that develop on this lane. As seen in **Photo 27.** when relatively low resistivity values (<14 ohm.m) and medium to high chargeability values (>10 msec) indicated as a strong alteration zone indicate an argillic alteration zone. When classified more specifically based on the geology of the research area, the alteration of the argillic zone can be divided into two, namely the smectite alteration and the illite alteration. Relatively high resistivity values (>24 ohm.m) and relatively low to medium chargeability values (<50,005 msec) indicate intrusion rocks. Relatively low resistivity (<14 ohm.m) and relatively low chargeability (<10 msec) indicate that there is clay in the area.

The eighth has a mineral zone between the -175m - 0m measurement benchmarks, due to a continuous structure based on the correlation between the filter analytic signal, first horizontal derivative, and second vertical derivative and resistivity values that are relatively medium to high (>14 ohm.m) and relatively medium to high chargeability values (>10 msec) which indicate that there are mineral zones on this lane.

Conclusions

From the results of the research, the following conclusions are:
1. Structure analysis using Analytic Signal, First Horizontal Derivative, and Second Vertical Derivative obtain structure, namely reverse fault and normal fault which is dominantly directed northwest-southeast.
2. Alteration analysis using the Time Domain Induced Polarization method supported by

geological data found argillic alterations (illite and smectite) with relatively low resistivity values (<14 ohm.m) and medium to high chargeability values (>10 msec) indicated as a strong alteration zone with sulfide mineral content. And also found propylitic alteration with relatively medium to high resistivity values (>14 ohm.m) and relatively medium to high chargeability values (>10 msec).
3. Correlation between magnetic response and electrical response (resistivity and chargeability), the gold mineralization zone is in 1st lane and 2nd lane between a distance of 600m to 800m measurement in the Southwest - Northeast direction and also in 5th lane and 6th lane between a distance of 0m to 200m measurement in the Southwest direction, 7th lane is on the measurement pole 0 m, and 8th lane between a distance of -200m to 0m measurement in the Southwest direction indicated by the value of high magnetic anomaly, high resistivity, and high chargeability, and the development of argillic alteration zones, namely illite and smectite.

* Corresponding Author: alimuddin.geofisika@eng.unila.ac.id
** ribkarebekka22@gmail.com
*** ordas.dewanto@eng.unila.ac.id
**** wicaksonoarief123@gmail.com
***** andi.kurniawan@antam.com

DAFTAR PUSTAKA

Angeles, C. A., Sukmandaru, P., and James, S. W. 2002. Geology and Alteration-Mineralization Characteristics of the Cibaliung Epithermal Gold Deposit, Banten, Indonesia. *Resource Geology Vol. 52 No. 4*, 329–339.

Bateman, A. M. 1981. *Economic Mineral Deposit*. New York: Jhon Wiley and Sons, Inc.

Blakely, R. J. 1995. *Potential Theory in Gravity and Magnetic Applications*. Sydney: Cambridge University Press.

Chen, G., Cheng, Q., Liu, T., and Yang, Y. 2013. Mapping local singularities using magnetic data to investigate the volcanic rocks of the Qikou depression, Dagang oilfield, eastern China. *Nonlinear Process in Geophysics Vol. 20 No. 1*, 501-511.

Corbett, G. J. 2002. Epithermal Gold for Explorationists. *AIG Journal – Applied geoscientific practice and research in Australia No. 67*, 8.

Corbett, G. J., and Leach, T.M. 1997. *SW Pasific Rim Gold and Cooper System: Structure, Alteration, and Mineralization*. Aucland: CMS New Zealand Ltd.

Cordell, L. E., and Grauch, V. J. S. 1985. *Mapping basement magnetization zones from aeromagnetic data in the San Juan Basin*. New Mexico: Utility of Regional.

Guilbert, J. M., and Park, C. F. 1986. *The Geology of Ore Deposits*. New York: W. H. Freeman and Company.

Guo, N., et al. 2019. Characterization of Illite Clays associated with the Sinongduo low sulfidation epithermal deposit, Central Tibet using field SWIR spectrometry. *Ore Geology Reviews*. 103-228.

Indratmoko, P., dkk. 2009. Interpretasi Bawah Permukaan Daerah Manifestasi Panas Bumi Parang Tritis Kabupaten Bantul DIY Dengan Metode Magnetik. *Jurnal*. Universitas Diponegoro Semarang.

Phillips, J.D. 1998. Processing and Interpretation of Aeromagnetic Data for the Santa Cruz Basin Patahonia Mountains Area, South-Central Arizona: U.S. *Geological Survey Open-File Report*, 02-98.

Pirajno, F. 1992. *Hydrothermal Mineral Deposits, Principles and Fundamental Concepts for the Exploration Geologist*. New York: Springer-Verlag.

Prihatmoko, S., and Idrus, A. 2020. Low-sulfidation epithermal gold deposits in Java, Indonesia: Characteristics and linkage to the volcano-tectonic setting. *Ore Geology Reviews 121*, 103-490.

Sutarto. 2004. *Petunjuk Praktikum Endapan Mineral Edisi Kedua*. Laboratorium Endapan Mineral. Jurusan Teknik Geologi, UPN Veteran Jogjakarta.

Telford, W. M., Geldart, L. P., and Sheriff, R. E. 1990. *Applied Geophysics, 2nd edition*. Cmbridge: Cambridge University Press.

Voudouris, P. 2019. Porphyry and epithermal deposits in Greece: An overview, new discoveries, and mineralogical constraints on their genesis. *Ore Geology Reviews 107*, 654–691

Appendix

Photo 7. Excel Processing IGRF Correction
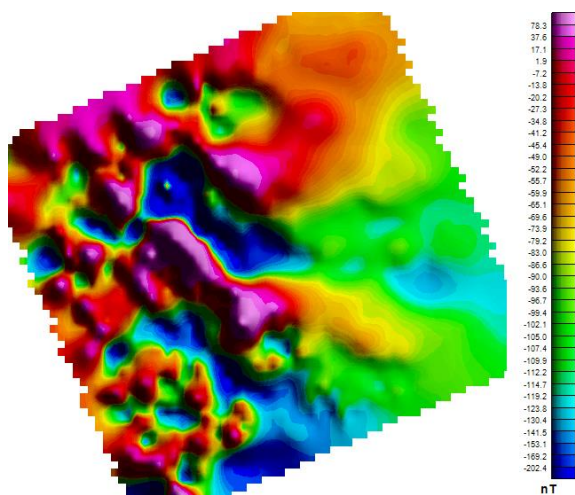
Photo 8. Magnetic Anomaly Intensity Contour before RTP
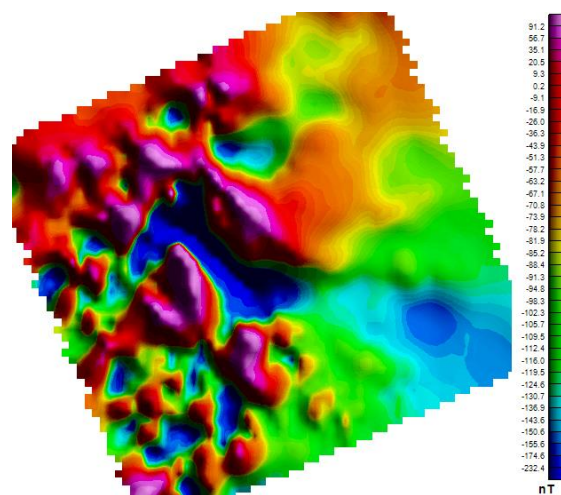
Photo 9. Magnetic Anomaly Intensity Contour after RTP

* Corresponding Author: alimuddin.geofisika@eng.unila.ac.id
** ribkarebekka22@gmail.com
*** ordas.dewanto@eng.unila.ac.id
**** wicaksonoarief123@gmail.com
***** andi.kurniawan@antam.com
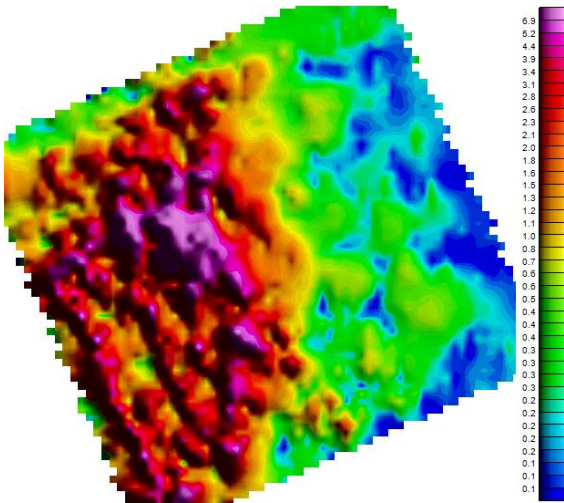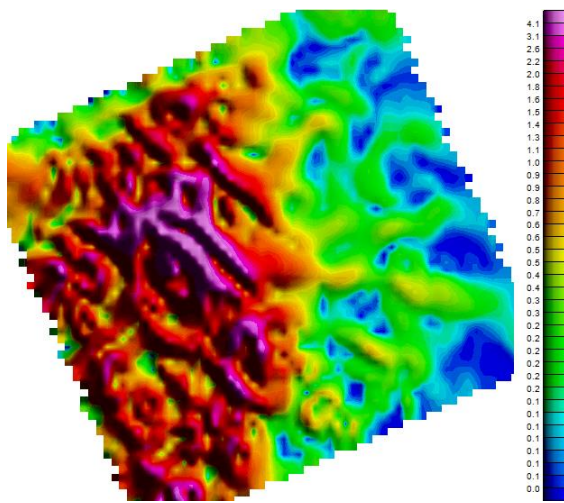
Photo 10. *Analytic Signal* Contours
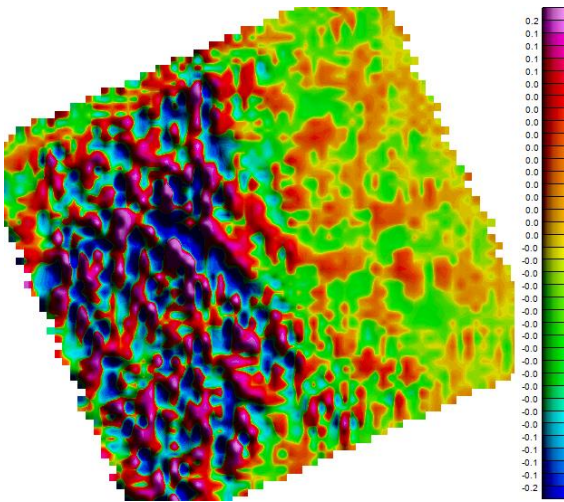

**Photo 11.** *First Horizontal Derivative* Contours

Photo 12. *Second Vertical Derivative* Contours

a.   b.   c.
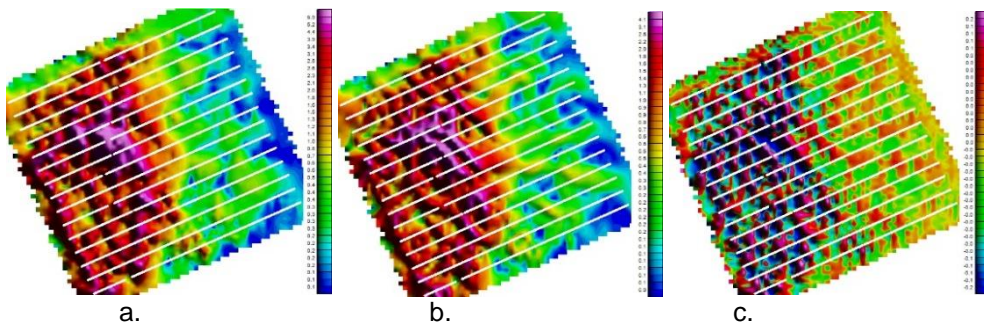
Photo 13. Slicing of The (a.) *Analytic Signal*, (b.) *First Horizontal Derivative,* dan (c.) *Second Vertical Derivative*

a.

b.

c.
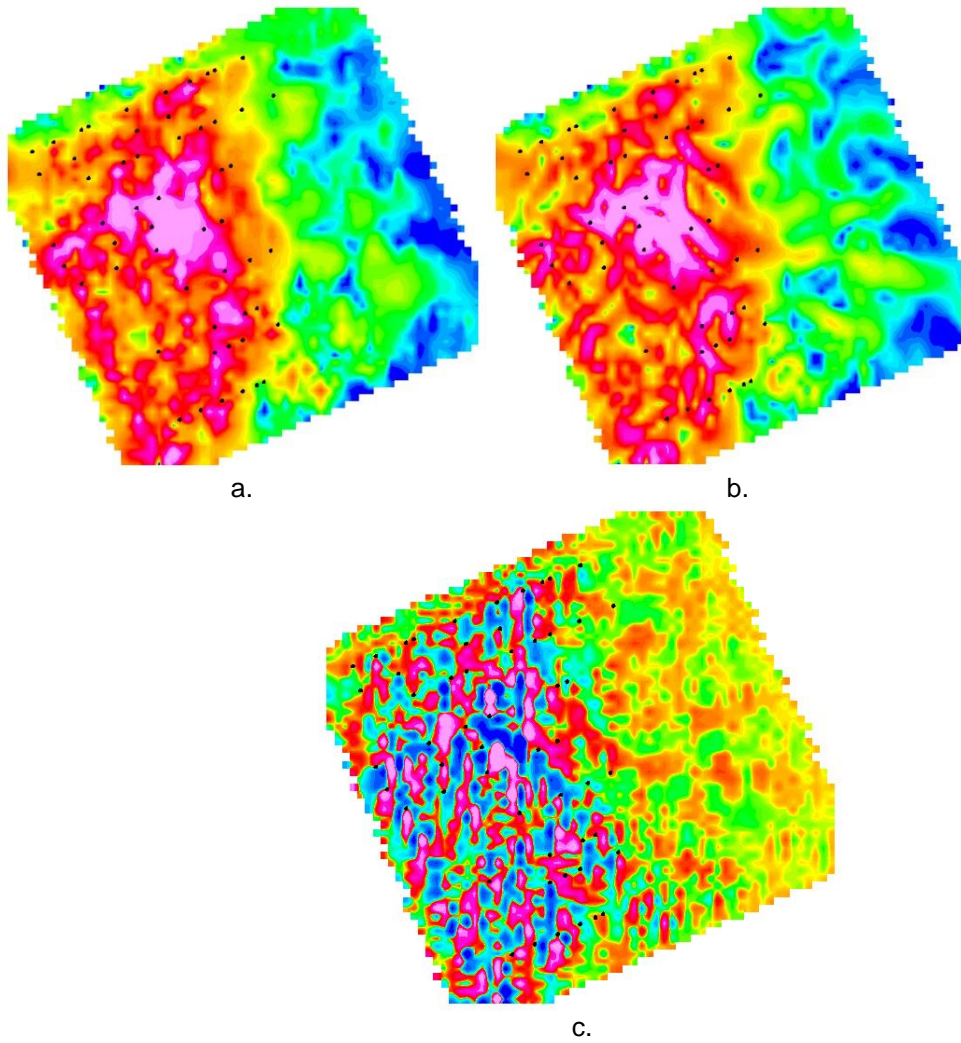
Photo 14. Structure Dots of The (a.) *Analytic Signal*, (b.) *First Horizontal Derivative,* dan (c.) *Second Vertical Derivative*
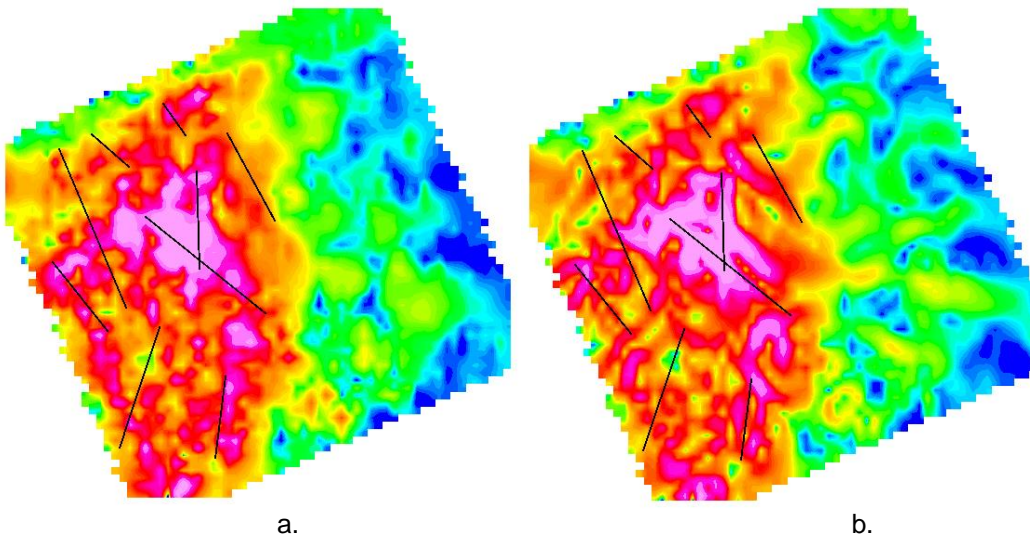
a.

b.

* Corresponding Author: alimuddin.geofisika@eng.unila.ac.id
** ribkarebekka22@gmail.com
*** ordas.dewanto@eng.unila.ac.id
**** wicaksonoarief123@gmail.com
***** andi.kurniawan@antam.com
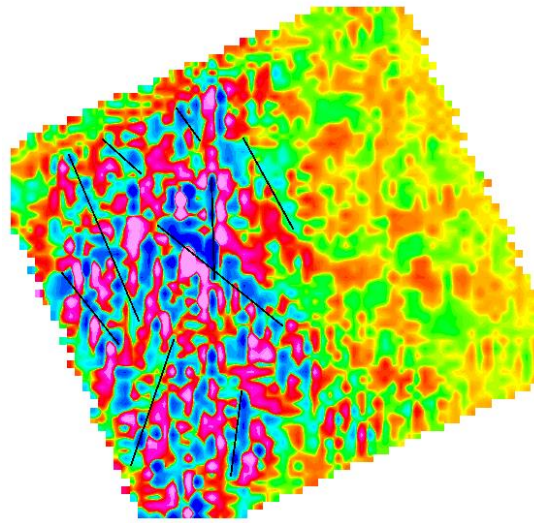
c.

Photo 15. Results of Structure Interpretation of The (a.) *Analytic Signal*, (b.) *First Horizontal Derivative,* dan (c.) *Second Vertical Derivative*
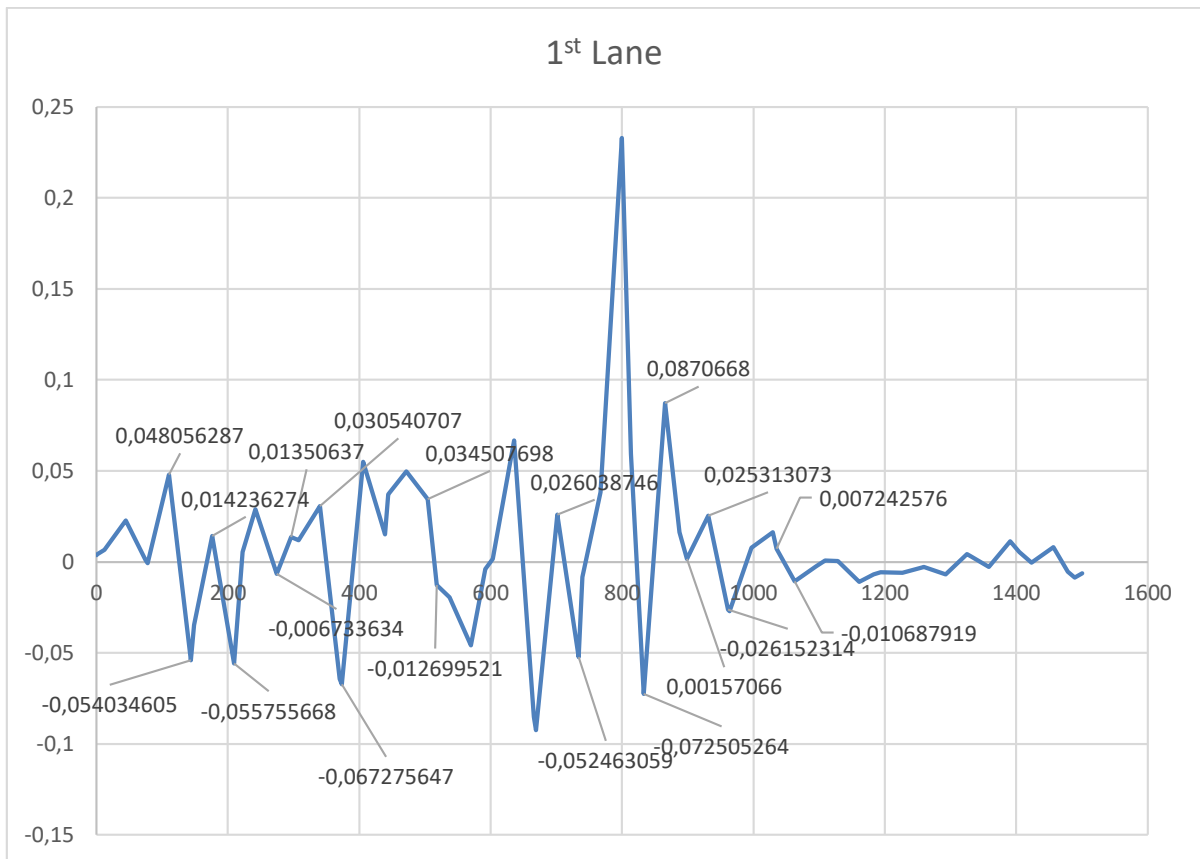
Photo 16. SVD Slicing Results Curve 1st lane
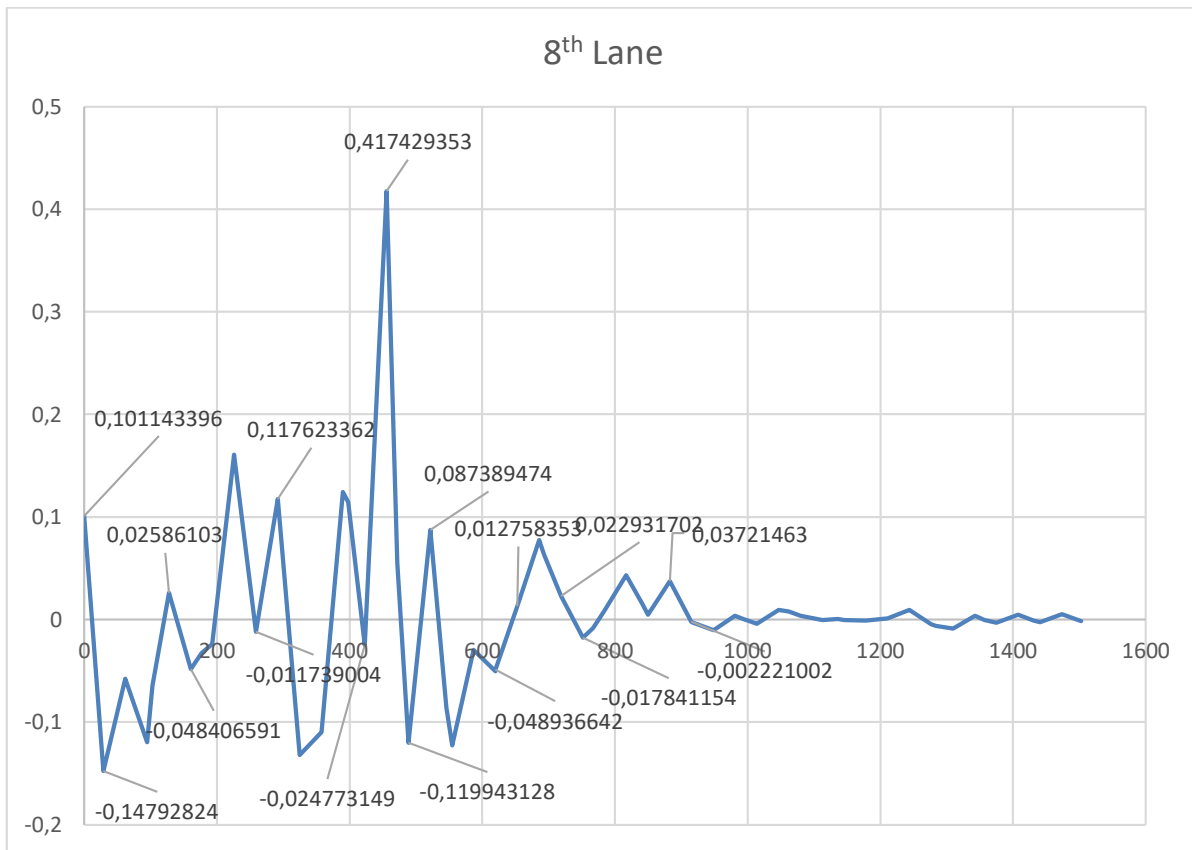
Photo 17. SVD Slicing Results Curve 8th lane

* Corresponding Author: alimuddin.geofisika@eng.unila.ac.id
** ribkarebekka22@gmail.com
*** ordas.dewanto@eng.unila.ac.id
**** wicaksonoarief123@gmail.com
***** andi.kurniawan@antam.com

Penampang 2D Resistivity
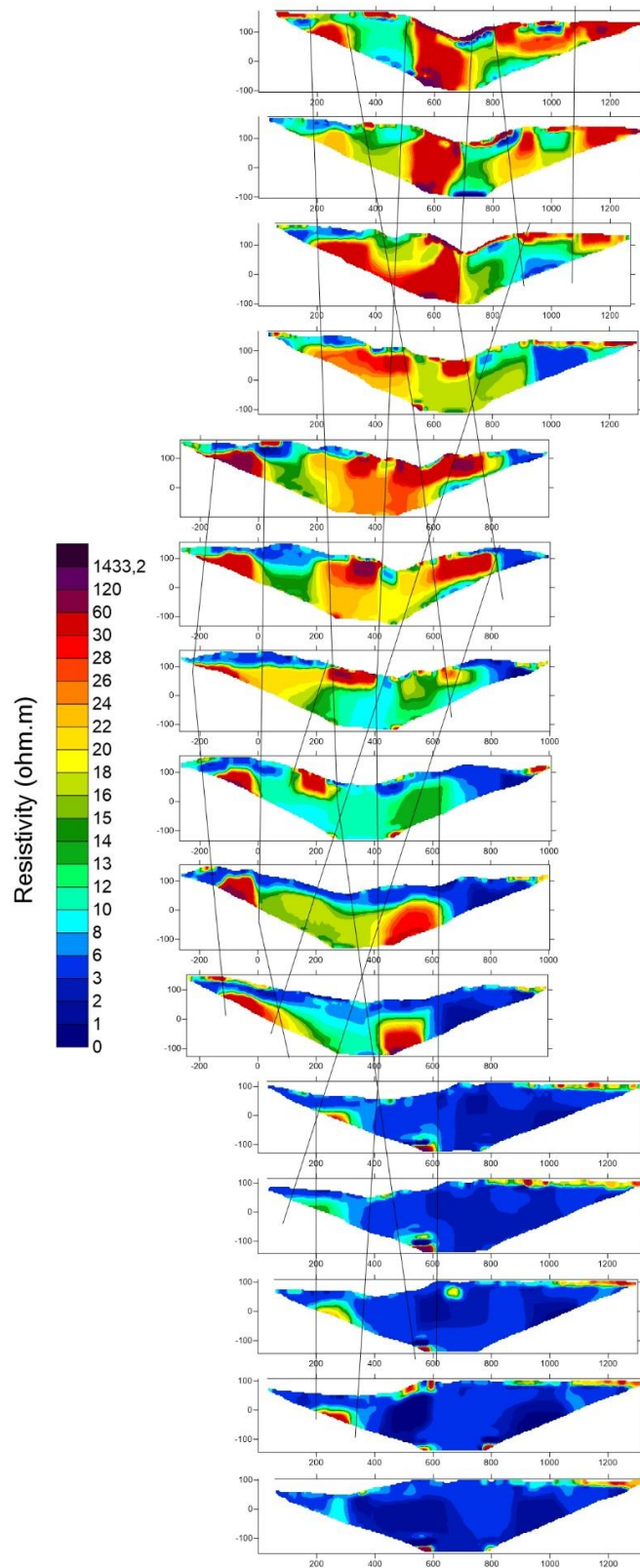
Photo 18. 2D Resistivity Section

Penampang 2D Chargeability
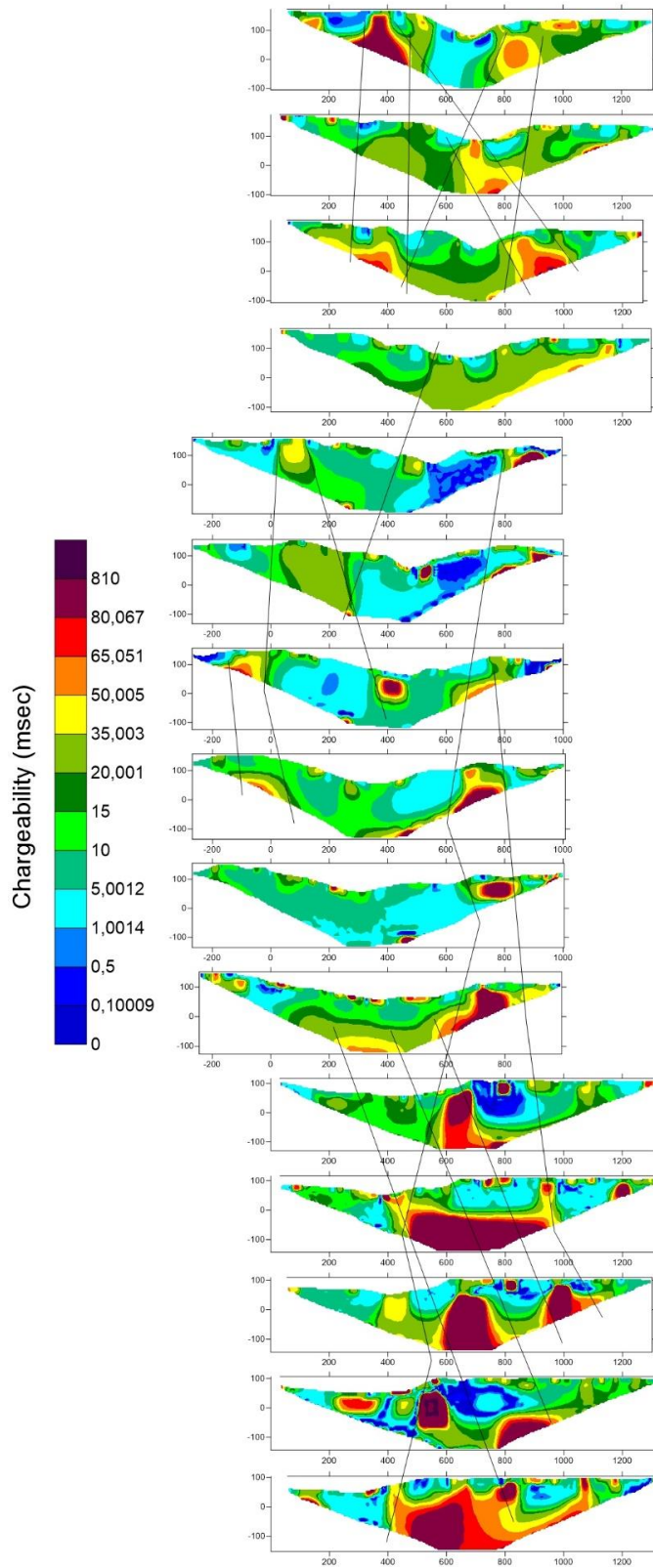
Photo 19. 2D Chargeability Section

* Corresponding Author: alimuddin.geofisika@eng.unila.ac.id

** ribkarebekka22@gmail.com

*** ordas.dewanto@eng.unila.ac.id

**** wicaksonoarief123@gmail.com

***** andi.kurniawan@antam.com
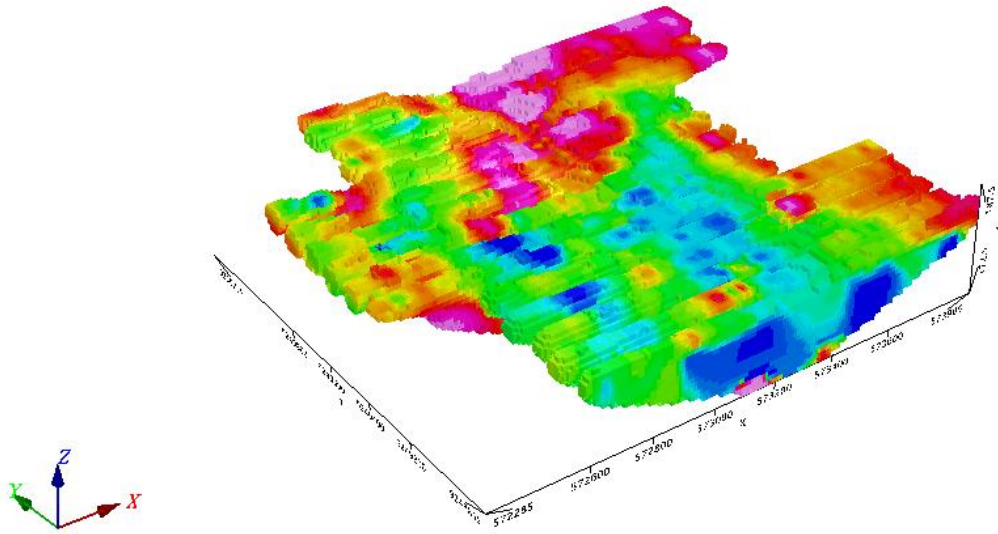
Photo 20. 3D Resistivity Section
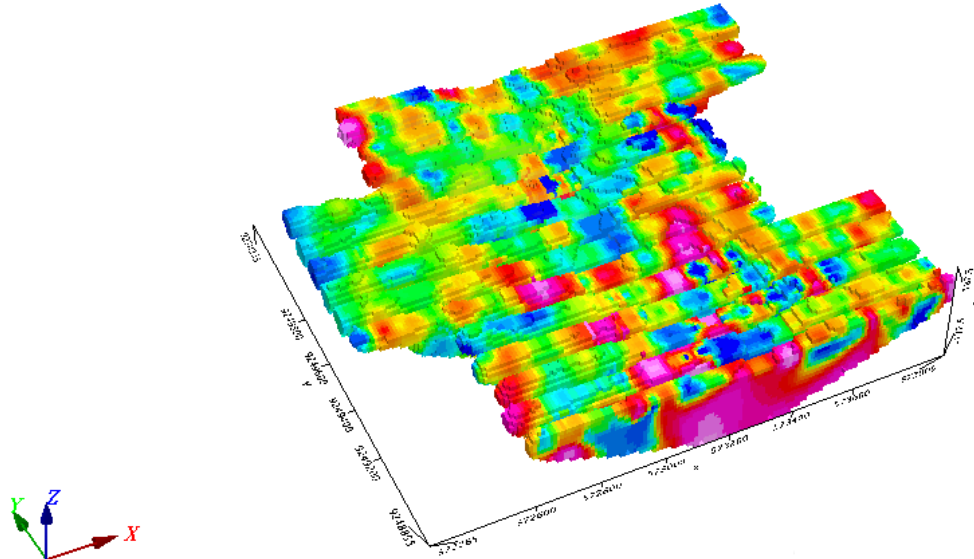
Photo 21. 3D Chargeability Section
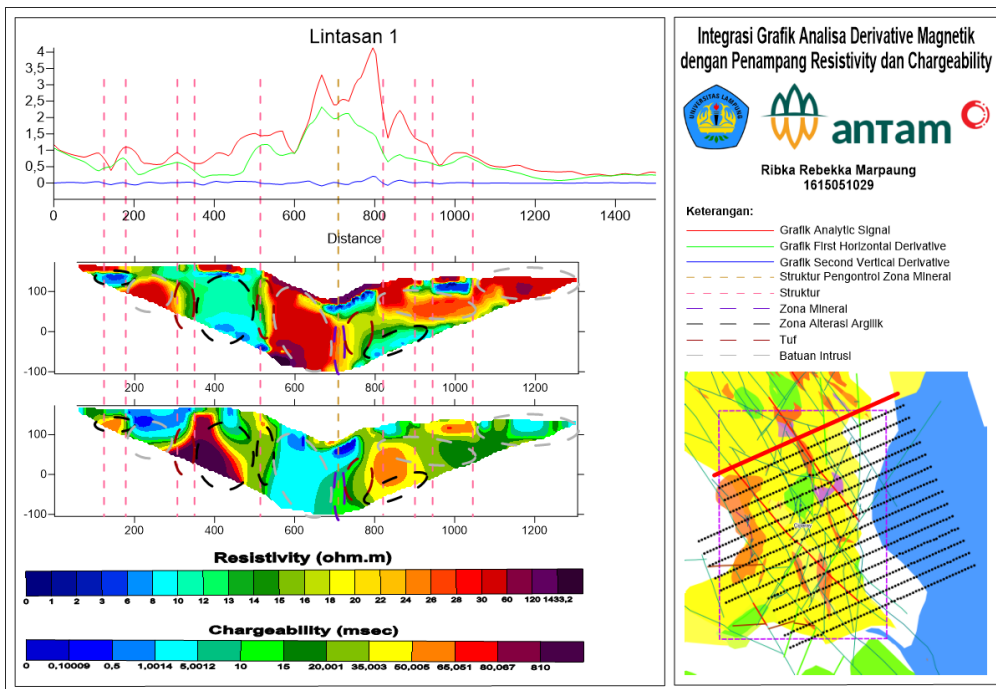
Photo 22. Correlation Between Geological Data, Magnetic Data and Time Domain Induced Polarization Data on 1ˢᵗ lane
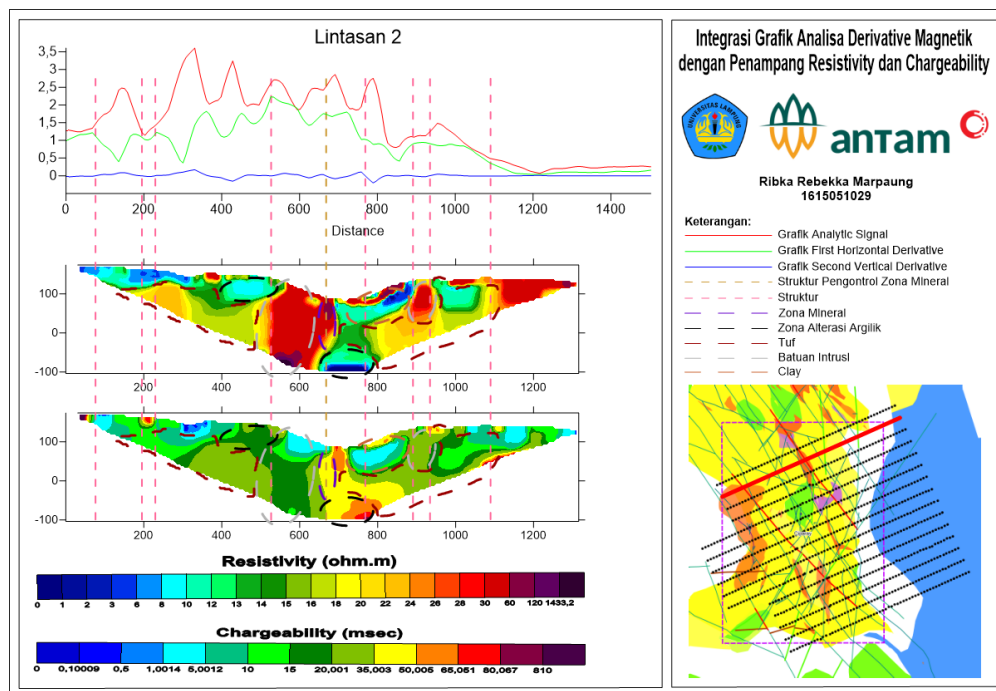
Photo 23. Correlation Between Geological Data, Magnetic Data and Time Domain Induced Polarization Data on 2ⁿᵈ lane

* Corresponding Author: alimuddin.geofisika@eng.unila.ac.id

**   ribkarebekka22@gmail.com

*** ordas.dewanto@eng.unila.ac.id

**** wicaksonoarief123@gmail.com

***** andi.kurniawan@antam.com
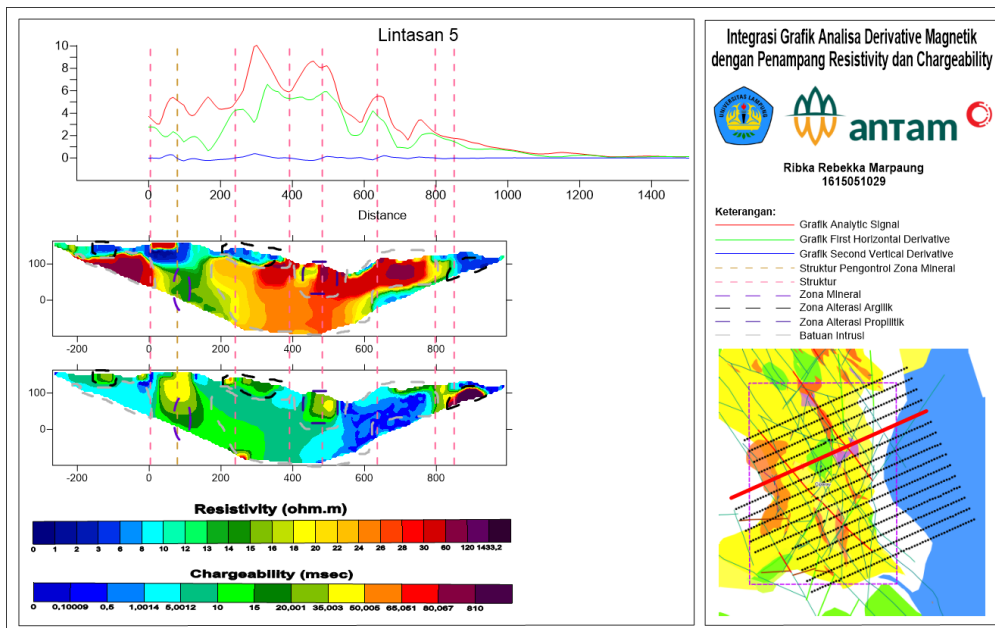
Photo 24. Correlation Between Geological Data, Magnetic Data and Time Domain Induced Polarization Data on 5th lane
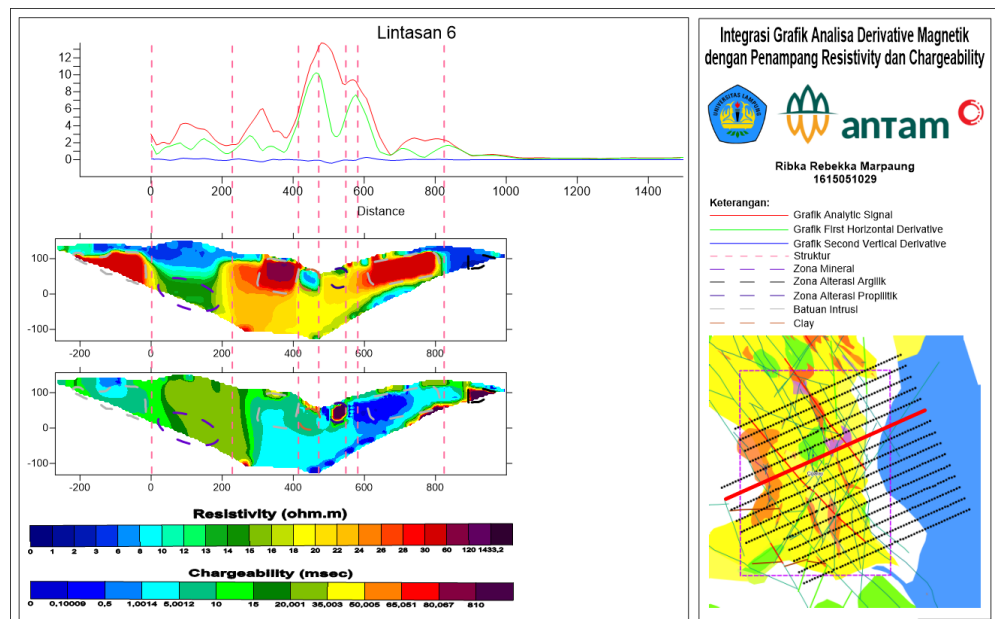

Photo 25. Correlation Between Geological Data, Magnetic Data and Time Domain Induced Polarization Data on 6th lane
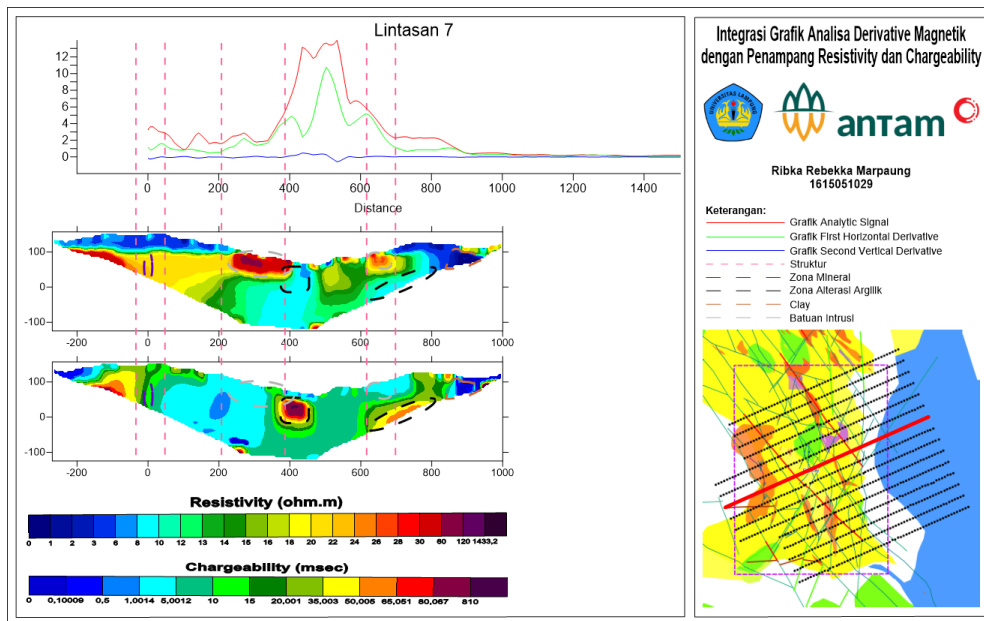
Photo 26. Correlation Between Geological Data, Magnetic Data and Time Domain Induced Polarization Data on 7th lane
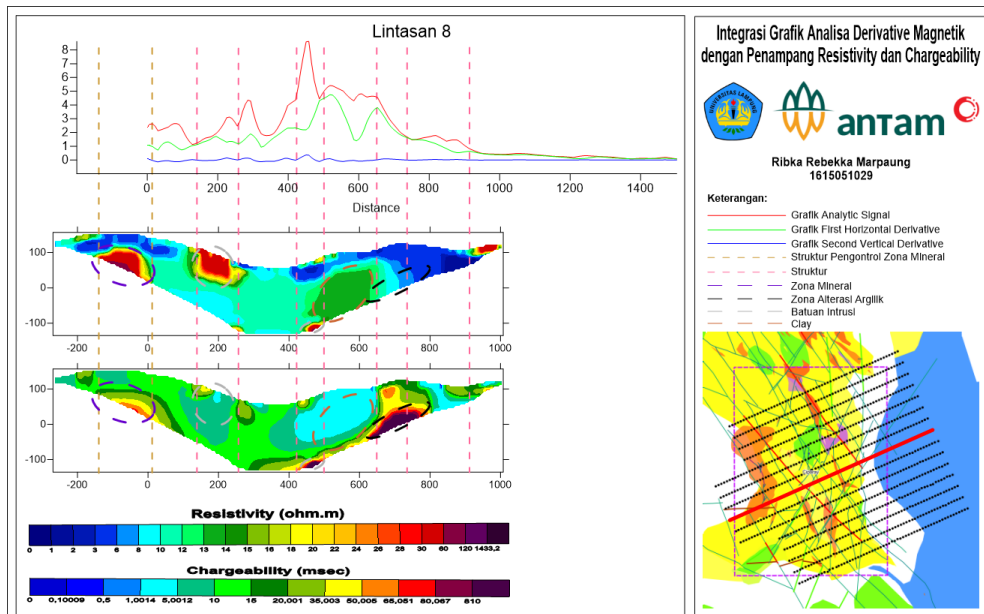

Photo 27. Correlation Between Geological Data, Magnetic Data and Time Domain Induced Polarization Data on 8th lane

* Corresponding Author: alimuddin.geofisika@eng.unila.ac.id

** ribkarebekka22@gmail.com

*** ordas.dewanto@eng.unila.ac.id

**** wicaksonoarief123@gmail.com

***** andi.kurniawan@antam.com